Development and Characterization of Custom-engineered and Compacted Nanoparticles as Calibration Materials for Quantification Using LA-ICP-MS

Journal:	*Journal of Analytical Atomic Spectrometry*
Manuscript ID:	JA-ART-02-2014-000054.R1
Article Type:	Paper
Date Submitted by the Author:	25-Mar-2014

Complete List of Authors:	Tabersky, Daniel; ETH Zurich, Department of Chemistry and Applied Biosciences, Laboratory of Inorganic Chemistry Lüchinger, Norman; nanoSRM (Nanograde AG), Rossier, Michael; nanoSRM (Nanograde AG), Reusser, Eric; ETH Zürich, Institute for Geochemistry and Petrology Hametner, Kathrin; ETH Zurich, Laboratory of Inorganic Chemistry Aeschlimann, Beat; ETH Zurich, Laboratory of Inorganic Chemistry Frick, Daniel; ETH Zurich, Department of Chemistry and Applied Biosciences Halim, Samuel; nanoSRM (Nanograde AG), Thompson, Jay; University of Tasmania, CODES Danyushevsky, Leonid; University of Tasmania, CODES Gunther, Detlef; ETH Zurich, Department of Chemistry and Applied Biosciences, Laboratory of Inorganic Chemistry

Development and Characterization of Custom-engineered and Compacted Nanoparticles as Calibration Materials for Quantification Using LA-ICP-MS

Daniel Tabersky[1], Norman Lüchinger[2], Michael Rossier[2], Eric Reusser[3], Kathrin Hametner[1], Beat Aeschlimann[1], Daniel A. Frick[1], Samuel Halim[2], Jay Thompson[4], Leonid Danyushevsky[4] and Detlef Günther[1]*

[1] ETH Zurich, Department of Chemistry and Applied Biosciences, Laboratory of Inorganic Chemistry, Wolfgang-Pauli-Strasse 10, 8093 Zurich, Switzerland

[2] nanoSRM (Nanograde AG), Laubisrütistrasse 50, 8712 Stäfa, Switzerland

[3] ETH Zurich, Department of Earth Sciences, Institute for Geochemistry and Petrology, 8092 Zurich, Switzerland

[4]CODES CoE and School of Physical Sciences, University of Tasmania, Hobart, 7001, Australia

*Corresponding author: D. Günther, E-mail: guenther@inorg.chem.ethz.ch, Tel.: +41 44 632 46 87, Fax: +41 44 633 10 71

TOC entry

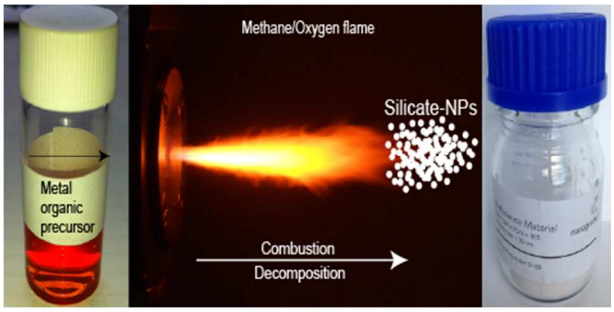

Flame spray synthesis was used to produce a nano-material with a customized composition.

Abstract

The flame spray technique was used to produce a nano-material with a customized composition. Liquid organic precursors of Si, Ca, Ti, Mg, Fe, Al in a similar concentration as the matrix of the well-known NIST SRM 610 glass standard were mixed with a selection of rare earth elements (Ce, Gd, Ho, Tb), precious metals (Ag, Au, Pd, Pt, Rh, Ru) and Pb at concentrations of approx. 400-500 mg/kg. The liquid precursor mixture was sprayed and collected as nano powder, compacted to pellets and analyzed by solution and laser-ablation inductively coupled plasma mass spectrometry. The bulk composition of the material was determined on several aliquots of the powder, either 25 mg or 50 mg. Electron microprobe analyses were carried out to further characterize the major element composition of the pressed nano-material. The pellet was ablated using different laser ablation systems with an aim of assessing the micro-scale homogeneity of the produced material.

The manufactured material is homogenous for major elements and REE's similar to the NIST glass (<5 % RSD). However, the distribution of the PGE's showed some larger spatial variation in the order of (<7.5%). In addition it is shown that contamination during production lead to heterogeneous distribution of Pb and Ag. Based on the results achieved for Ru, Rh, Pd, Au and Pt, Mg, Ti, Fe, which are either absent or not available in sufficient concentration levels in NIST glass it is demonstrated that flame spray synthesis allows producing suitable customized matrix-matched calibration materials for micro-analytical techniques.

1 Introduction

State-of-the-art microanalytical methods, such as Laser Ablation Inductively Coupled Plasma Mass Spectrometry (LA-ICP-MS), Electron Probe Micro Analyzers (EPMA), Secondary Ion Mass Spectrometry (SIMS), and synchrotron radiation induced X-Ray fluorescence are widely applied in research and industry. Suitable reference/calibration materials are pivotal for the evaluation of the analytical accuracy in the application of the aforementioned techniques. The glass series of NIST SRM 61x have been the most commonly applied external reference material in LA-ICP-MS[1,2] and in most quantification strategies they are used in conjunction with internal standardization to correct for matrix-dependent ablation rates[3,4]. However, the NIST SRM 61x standards were intended for quality control and calibration in the bulk analysis of glasses and only about 100 kg were produced in the 1970s[5]. Though intended for quantification of large test portions, the NIST SRM 61x have been transferred to microanalytical tasks, usually by determining "accepted" values for those materials[6–12], which are summarized in the GeoReM database[10,13]. Heterogeneities have been reported for some sample charges[8,14], and it was indicated that element-dependent rim enrichments of up to 30% may occur. The composition of NIST SRM 61x is different to natural samples. Geologically relevant elements such as Ti, Fe and Mg are present in low mass fractions only and thus not matching the natural abundances of those elements typically required for the quantification of minerals. Consequently, the NIST SRM 61x series is not well suited for calibration of geological samples[15]. Moreover, every element not present in the NIST glass series are considered to be difficult to analyze, since a very limited number of other reference materials are available. For example, elements such as Rh, Ru, Pd, Pt (Platinum Group Elements, PGEs) and Au are either absent or present in very low concentrations.

Two approaches for the preparation of micro-analytical reference materials are employed by the U.S. Geological Survey[16]. In the first approach, which is similar to the production pathway of NIST SRM 610[5], a powdered material is melted in a high-temperature furnace and then flash-cooled to prevent crystallization. The resulting glass-like material commonly suffers from losses of volatile elements (*e.g.* Au, Ag, Ru, Tl) or elements, which alloy with the Pt-crucibles (*e.g.* Re), as was observed during the production of the NIST 61x series. In a second approach, a chemical precipitation procedure is used to produce a synthetic material with a well-defined elemental composition at predetermined concentrations, with a homogeneity given by the particle size distribution of the powder. The aforementioned approaches for the preparation of solid-state calibrants for microbeam techniques deliver only a limited homogeneity and compositional range, and are subject to tight restrictions in

the possibilities to adapt analyte/matrix composition to a particular application of interest. Since most microbeam techniques currently provide information at a scale smaller than 5 micrometer, and aim at an even higher spatial resolution, new reference materials homogenous at this scale are required.

Within the last several years, nanoparticle characterization has gained a lot of attention and various analytical approaches have been proposed to determine their stoichiometry. For example, nanoparticles of a wide range of compositions can be synthesized in a controlled way using bottom-up techniques, such as flame spray synthesis[17–27]. Based on that technology we tried to optimize the production approach to synthesize a new reference material. Selected elements were dissolved in an organic liquid precursor, which was subsequently sprayed and combusted, producing nanoparticles with sub-micron size distribution. This synthesis approach yielded a complex solid solution of all metal elements in form of nanoparticles of 10-50 nm, far below the commonly utilized spatial resolution in LA-ICPMS experiments.

For this proof-of-concept study we produced a modified NIST SRM 610-like material characterized by higher concentrations of Mg, Fe, and Ti (in the single wt%-range) and added PGE, Au, Ce, Gd, Ho, Tb and Ag at concentrations between 300 – 1000 ppm. The suitability of the novel solid material with customized composition as a calibration standard for LA-ICPMS was investigated with respect to ablation behavior and homogeneity.

2 Material and methods

Flame spray synthesis

All starting materials used were of high purity. Nanoparticles were synthesized by flame spray synthesis using a metal organic precursor containing all the elements to be present in the final product[27]. For the preparation of the precursor, corresponding portions of the (single element) metal organic solutions were combined so that they were fully miscible in Xylene. The detailed composition of the individual precursor composition cannot be given in more detail, because it represents intellectual property of nanoSRM (Nanograde AG). The metal organic precursors were filtered through a 0.45 um PTFE syringe filter and fed (5 mL min^{-1}, HNP Mikrosysteme, micro annular gear pump mzr-2900) to a spray nozzle, dispersed by oxygen (7 L min^{-1}, PanGas tech.) and ignited by a premixed methane-oxygen flame (CH_4: 1.2 L min^{-1}, O_2: 2.2 L min^{-1}). The off-gas was filtered through a glass fiber filter (Schleicher&Schuell) by a vacuum pump (Busch, Seco SV1040CV) at about 20 m^3 h^{-1}. The obtained nanopowder was collected from the glass fiber filter and stored in glass vials. Further information about flame synthesis and its capabilities can be found in (Ref.[27]). Aliquots of about 100-400 mg were pressed at 10 tons for about 10 minutes to disks of 13 mm in diameter using a conventional pill press. For this proof-of-principle study, a material composed of SiO_2, Al_2O_3, Fe_2O_3, TiO_2, MgO, Na_2O and CaO in concentrations of approximately 73, 2, 1.8, 2.2, 1.8, 7.5 and 11.5 wt%, respectively, was produced. Ag, Au, Pt, Pd, Ru, Rh, Ho, Tb, Gd, Ce were added at concentration levels between 300-1000 mg/kg.

Digestion and wet chemical analysis

At ETH, pressed pellets were crushed and pulverized. Subsequently, amounts of 50 mg were weighed into PTFE digestion vials and dissolved by microwave-assisted digestion on an ETHOS digestion system (MLS GmbH, Leutkirch, Germany). A simultaneous digestion of 9 samples was possible on the system used. 50 mg of the nanoparticle powder (n=5), one digestion blank, one laboratory fortified blank at 100% of the expected concentrations and two laboratory fortified matrix spikes at +100% and +200% of the expected concentrations were digested. For digestion, an acid mixture of 10 mL HCl, 3 mL sub boiled HNO_3 and 1 mL HF were utilized. The microwave system used offered adjustable power, but no control over temperature and pressure. The microwave program was 450W for 10 minutes and 250 W for 30 minutes similar to previously published procedures[28]. In a second microwave step, 10 mL of a saturated boric acid were added to the

digestion vials and 300 W were applied for 10 minutes. Solutions were then diluted in 2% HCl (v/v) up to a final weight of 50 g.

For analysis, 200 µL of each digest were diluted with 2 % (v/v) HCl to 20 g. For internal standardization, 200 µL of an internal standard solution containing 500 ng/g each of Lu, Cs, In, Sc, Re, Sb, and Ir was added to the sample solution before it was diluted up to the final volume. The internal standard closest to the analytical mass of interest was chosen. For external calibration in SN-ICP-MS, commercially available standard solutions were used for all elements. In addition, analyte specific spikes were conducted to correct for potential element specific losses during the digestion procedure.

Concentrations were determined using an ICP-SF-MS (Element2, Thermo Fisher Scientific, Bremen, Germany) with an Aridus I (CETAC, Omaha, USA) desolvation unit as sample introduction system and an autosampler (ASX-100, CETAC, Omaha, USA) for automated analysis. The system was operated at medium resolution ($m/\Delta m=4000$) with a 100% mass window, 20 samples per peak with a dwell time of 10 ms each and 50 replicates per measurement. Calibration standards and samples were introduced into the desolvation system using a self-aspirating, micro-concentric PFA nebuliser (PFA-ST, Elemental Scientific, Omaha, USA) with an nominal uptake rate of 50 µL min^{-1} and a sample and auxiliary gas flow of 1.20 L min^{-1} and 0.80 L min^{-1} respectively.

At UTAS, the pulverised powders were analysed for Ce, Gd, Tb, Ho, Rh, Pd, Ag, Pt and Au on an Agilent 7700x quadrupole ICP-MS. Calibrations were based on 1 ng/g, 5 ng/g and 10 ng/g mixed element solutions. ^{187}Re was used for internal standardisation. NIST SRM 610 powder and NIS3 powder[29] were analysed for quality control. NIST 610 was used to assess and correct for matrix effects and the efficiency of digestion for Ag, Ce, Gd, Tb and Ho, whereas NIS3 was used for Rh, Pd, Pt and Au. Corrections required for REE and Ag were negligible, whereas corrections for PGE were 10-20 per cent.

Two different digestions were performed. In both runs each sample was run in duplicates. For the first run, 25 mg of the sample were first dissolved in a mixture of 2 mL HF and 2 mL HNO_3 and then heated to near dryness. The samples were then dissolved in 1 mL HNO_3 and heated to near dryness again. The final dilution (50,000 times) was performed in two steps. The first step involved dissolving the sample in 100 g of 4% Aqua Regia (HCl : HNO_3 at 3:1) and then during the second step 4 mL of the solution were diluted in 2% HNO_3 to 50 g. For second run, HCL was added to the

first two digestion steps. The first step involved 2 mL HF, 1 mL HNO_3 and 1 mL HCl. The second step involved 1 mL HNO_3 and 1 mL HCl. The last two steps were the same as during the first run.

The results are presented in Table 2.

LA-ICP-MS

An ArF excimer laser system (GeoLas Compex, MicroLas, Göttingen, Germany) working at 193 nm with a pulse duration of 15 ns and a homogenized beam profile was used for ns-LA-ICPMS together with an Elan 6100 DRC + (Perkin Elmer, Waltham, MA, USA). Crater sizes of 20, 40, 60, 80 μm, respectively, and a fluence of 22 J/cm^2 were applied. The repetition rate was set to 5 Hz. The aerosol was transported with a helium carrier gas flow rate of 1.2 L/min. The ICP-MS system was operated at a power of 1380 W, nebulizer and auxiliary gas flow of 0.75 to 0.85 L/min (spot analysis and line scan, respectively) and a plasma gas flow of 17.5 L/min argon. The dwell time of the ICP was set to 10 ms per isotope, which resulted in 0.611 seconds per sweep. In addition to the single spot ablations, line scans were employed utilizing a crater size of 44 μm, a repetition rate of 10 Hz, a scan speed of 10 μm/s, and a fluence of 33 J/cm^2. Prior to each measurement series, all samples were placed inside a standard cylindrical ablation cell (V = 63 cm^3). NIST SRM 610 was used as calibration material. In addition, USGS BCR-2G and USGS GSE-1G were used as additional quality control for the REE and Pb. The LA-ICP-MS-signals were background corrected and integrated from the beginning to the end of the ablation signal (approx. 60 s) according to ref[30]. Concentrations (% m/m of all elements as oxides) were then normalised to 100%. $^{42}Ca^+$was used for internal standardization. To validate the use of this normalization procedure, major element data were determined by EPMA.

At UTAS, the instrumentation involves a Resonetics RESOlution S-155 laser ablation system coupled to an Agilent 7500cs quadrupole mass-spectrometer. RESOlution is equipped with a Coherent 193 nm excimer laser with a pulse width of ~ 20 ns. S-155 is a constant geometry, two chamber, large volume ablation cell. Analyses were performed in an atmosphere of pure He at a fluence of 3.5 J/cm^2, using a repetition rate of 10 Hz and laser beam sizes of 19 μm, 47 μm and 89 μm. The He carrier gas flowing at a rate of 0.35 L/min was mixed with Ar carrier gas (1.05 L/min) immediately after the ablation chamber. Mass-spectrometer was tuned for low oxide production (Th/ThO < 0.15%) and enhanced sensitivity for heavy masses. Dwell time for each isotope was set to 10 ms, resulting in the total sweep time of ~ 0.4 s. Analyses were performed in two modes, ablation at a fixed location and rastering, with the main focus on assessing the uniformity of particle compositions and homogeneity of element distribution within the material. In the raster mode, the

sample was moving under the laser beam with a rate equal to the beam diameter per second, thus resulting in every location along the beam path being ablated 10 times.

EPMA and SEM

For the analyses of major elements of the pressed silicate nanoparticles, an electron probe microanalyzer JEOL JXA 8200 equipped with five wavelength dispersive X-ray spectrometers (WDS) and an energy dispersive spectrometer (EDS) was used. The pressed pill was carbon coated (~20 nm) and connected with conducting silver to ground potential. Following operation conditions were applied: beam current of 20 nA at 15 kV acceleration potential, 20 μm spot sizes at a spacing of 200 μm. The analysis involved the measurement of Si, Ca, Na, Al, Fe, Mg, and Ti. Oxygen was calculated from the charge balance. External standards used were natural and synthetic oxides. All analyses are corrected for dead time of the detector, instrumental drift and background. For the evaluation of homogeneity, the data was summarized in grids, which each consisted of 10 data points in line. All values were normalized to 100 wt%-oxides and disregarded when the original sum was below 50%, as low totals are caused due to the porosity.

Images of particles enriched in precious metals were taken with a Hitachi SU-70 field emission scanning electron microscope Field Emission SEM (Central Science Laboratory, University of Tasmania), using 1.5 kV and 10-15 mm working distance, resulting in ~ 1.6 nm pixel resolution. An Oxford AZtec 2.1 Inca Energy 350 EDS system with XMax80 SDD detector was used to determine the composition of the particles.

3 Results and discussion

3.1 Compacting nanoparticles

The nanoparticles were compacted by conventional pill pressing method (product shown in Fig. 1). It needs to be noted that the amount of the proof of principle batch supplied to two different laboratories and used for solution analysis was too small to study the optimum compacting conditions in more detail. The small average single particle diameter (typical values reported for flame synthesis are on the order of 10-50 nm[26,31]) allowed for producing a pellet without the use of additional binders. Typically, about one minute is necessary to receive stable pressure conditions inside of the press. The produced pellets were mechanically stable and could be handled similar to a glass. However, the surface roughness seen in Fig 1 a) indicates the other sample preparation procedures need to be applied when using these materials for very high spatial resolution techniques. Inspection of the final material revealed no visible zonation.

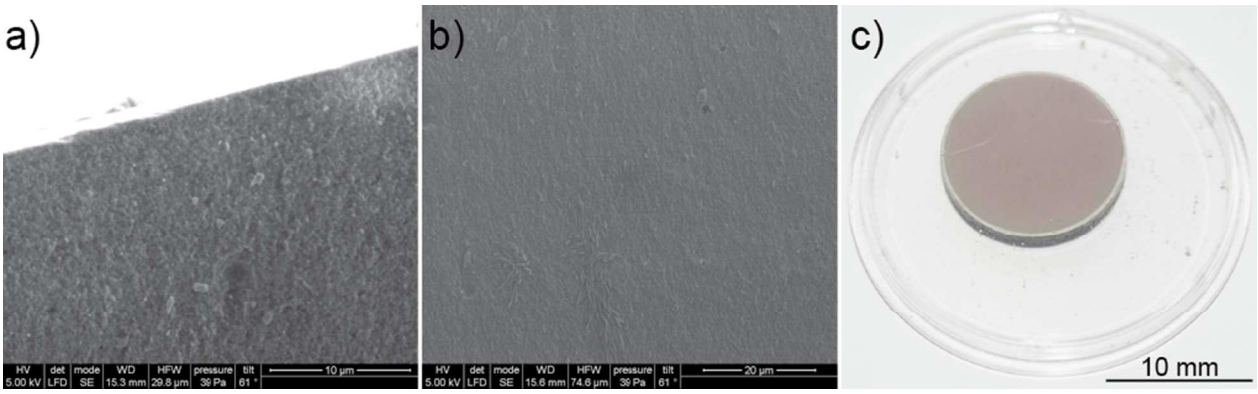

Fig. 1 Compacted nanoparticles. In Fig 1 a/b electron microscope pictures of the pressed nanoparticle powder are shown. Fig 1 a) is taken from the side whereas Fig 1 b) shows the top of the pellet. The final pellet as used for laser ablation is shown in Fig 1 c).

3.2 Preliminary assessment of concentration and homogeneity

A homogeneous distribution of major elements is a prerequisite for the correction of matrix-dependent ablation yields, matrix effects and instrumental drift to obtain accurate quantification by LA-ICP-MS.

In this study, EPMA was used to determine the major element concentration across the pressed pellet at 20 μm beam diameter using a spot to spot distance of 200 μm. Mass fractions for Al_2O_3, Na_2O, TiO_2, CaO, Fe_2O_3, SiO_2, MgO, standard deviations of the mean, RSDs, and counting errors are summarized in Table 1. One possible indicator for a homogeneous distribution of major

elements is, when the relative standard deviation of concentration determinations of each analyte is smaller than the analytical uncertainty[12]. The RSDs of the concentration of all major elements (n=437) within the newly synthesized material ranged from 0.4-3.31 %. Using the approach reported in ref.[12], it can be seen that the RSDs for Si, Ti and Al are indistinguishable from counting errors of EPMA, which allows to conclude that the major element concentration of these elements are homogeneous at a spatial resolution of 20 μm. However, the RSDs determined for Ca, Fe, Mg and Na are slightly above the criteria for homogeneity requiring further investigations. For example, the crucial surface flatness for EPMA was not studied in detail, but it might be possible that the partially higher RSD's were caused by surface effects and/or voids. According to Wilson *et al.*[32], materials providing an RSD of less than 4 % measured for all major elements qualify as reference material for LA-ICPMS studies.

Table 1 Major element composition of the nano material determined by EPMA and SN-ICP-MS.

	EPMA				ICP-MS	
Major Elementoxide (% m/m)	Mean (n=437)	Standard deviation	RSD (%)	Counting error (%)	Mean (n=5)	Standard deviation
Al_2O_3	2.02	0.05	2.16	2.21	2.01	0.02
Na_2O	6.66	0.17	2.65	1.42	7.6	0.1
TiO_2	2.30	0.05	2.32	2.38	2.26	0.02
CaO	11.38	0.16	1.43	0.42	11.4	0.6
Fe_2O_3	1.88	0.06	3.31	2.29	1.85	0.03
SiO_2	74.2	0.3	0.37	0.34	---	---
MgO	1.72	0.05	3.00	2.70	1.71	0.01

In addition to EPMA data, the results were independently determined by SN-ICP-MS. Five portions (50 mg) of the nanomaterial were digested in the Laboratory of Inorganic Chemistry (ETH Zurich) and concentrations of all elements (major, minor) were determined. As some elements have a high tendency to form insoluble fluorides, they were determined by standard additions in the digestion vials. The concentrations of the major elements determined by SN-ICP-MS are also shown in Table 1 for a direct comparison to the data determined by EPMA. The two data sets are identical within 1 σ uncertainty. However, the uncertainties associated with analyses using SN-ICP-MS were larger when compared to analyses using EPMA due to the difference in the number of independent determinations (n=5 *vs.* n=437). The average concentration for Na determined by EPMA was ~ 8% lower when compared to SN-ICP-MS. EMPA determines a generally lower Na_2O concentration because of possible migration or volatilization of sodium during electron excitation [33–35].

To investigate the general capability of flame synthesis to produce homogeneous nanomaterials, matrix compatible elements, such as Gd, Ho, Ce and Tb were also incorporated into the matrix and

quantified using solution nebulisation (UTAS and ETH) and results are summarized in Table 2. The REE data (average) determined in the two labs, using 25 and 50 mg of the powder are indistinguishable within error, showing no indication for inhomogeneous distribution in the mg range. This is also supported by the standard deviation of the 4 and 5 individual digests (Table 2).

Table 2 Results of digestions determined by SN-ICP-MS. Note the 1 σ uncertainty is given in brackets. Elements noted with a * were determined using standard additions at ETH.

Element (mg/kg)	Isotope used	ICP-MS ETH	ICP-MS UTAS	Preferred	N
Ru	101	325 (3)		*325 (5)*	5
Rh*	103	500 (7)	494 (4)	501 (5)	9
Pd	105	476 (4)	483 (2)	480 (5)	9
Ag	107	908 (34)	976 (13)	*942 (37)*	9
Ce*	140	403 (6)	400 (1)	402 (6)	9
Gd	157	407 (5)	395 (2)	401 (6)	9
Tb	159	314 (3)	315 (3)	315 (4)	9
Ho*	165	357 (3)	348 (5)	353 (7)	9
Pt	195	389 (4)	374 (2)	381 (5)	9
Au	197	497 (5)	500 (16)	499 (17)	9
Pb	208	560 (4)	580 (2)	570 (5)	9

The same digests as described above were used to quantify the PGE elements (Pd, Pt, Rh, Ru), Ag, Au and Pb doped to the nano-powder. These measurements provided agreements between the two labs within 3.8 % and the RSD's of multiple digests were Au 1.0 %, Pt 1%, Rh 1.4%, Pd 0.8%, Ru 1.2 %, and Pb 0.7 %, respectively. However, the values for Ag (8 % difference between the two laboratories) and 4 % RSD of multiple digests indicated already that this element shows significant higher variation when compared to the other added elements. Based on the results of both laboratories, the preferred values have been derived and are summarized in Table 2. Values given in italic are information values only.

3.3 Microanalytical assessment by laser ablation

Quantification of PGEs using LA-ICP-MS is difficult because of (i) potential fractionation effects and (ii) the lack of calibration standards. Available materials that could be used for quantification provide an uncertainty exceeding the requirements of this study. Silicate matrices containing 300-500 mg/kg have not been produced so far due to the loss of these elements during production, as discussed above.

To assess the level of homogeneity of the element distribution within the material, spatially resolved transient signals were recorded by LA-ICP-MS in two different laboratories. Crater diameters of 20-80 μm (ETH) and 19-87 μm (UTAS) were applied to characterize the material in single hole drilling and 40 μm and 47 μm were used in line scan mode, respectively. The data shown for the line scan mode (Fig. 2) indicate that all elements added as trace elements were successfully implemented into the matrix. However, the variations in the transient signals within the order of 7 % (1 σ) show a) differences between the REEs, PGE and Pb ratios to Ca across the sample and b) significant differences in the frequency of locally enriched nanoparticles (spikes). The Ag and Pb signals, as already noticed in the solution data, show the highest variability and number of spikes. The length of the signal spikes for Ag and Pb indicate micro-agglomerates, which are most likely to be caused by contaminations of the spraying reactor, since the spraying unit is regularly used for the production of PbO and other materials. These spikes cause deviations of 13% for Pb (in both laboratories) and 17% for Ag, respectively. This explanation is further supported by the W signal intensity, an element detected, but not added to the precursor mixture (see W signal in supplement information). These findings indicate that further production of such materials requires extensive cleaning of the reactor unit to avoid carry over effects.

These micro-agglomerates have to be distinguished from single element particles, which have also been obtained for most of the PGE's. However, they were absent for REE's and major element oxides. Fig. 3 shows an enriched Pd and Pt nanoparticle on the surface of the pressed pellet. The total number of these spikes is low and had no influence on the solution nebulisation data. However, their occurrence amounts to an RSD of 7 %. A more detailed analysis of the transient signals indicate that the Ru/Ca ratio shows some layer structures, which is evidence for a heterogeneity within the material. The RSD determined are in the order of <7.3% for all elements (except Ag and Pb).

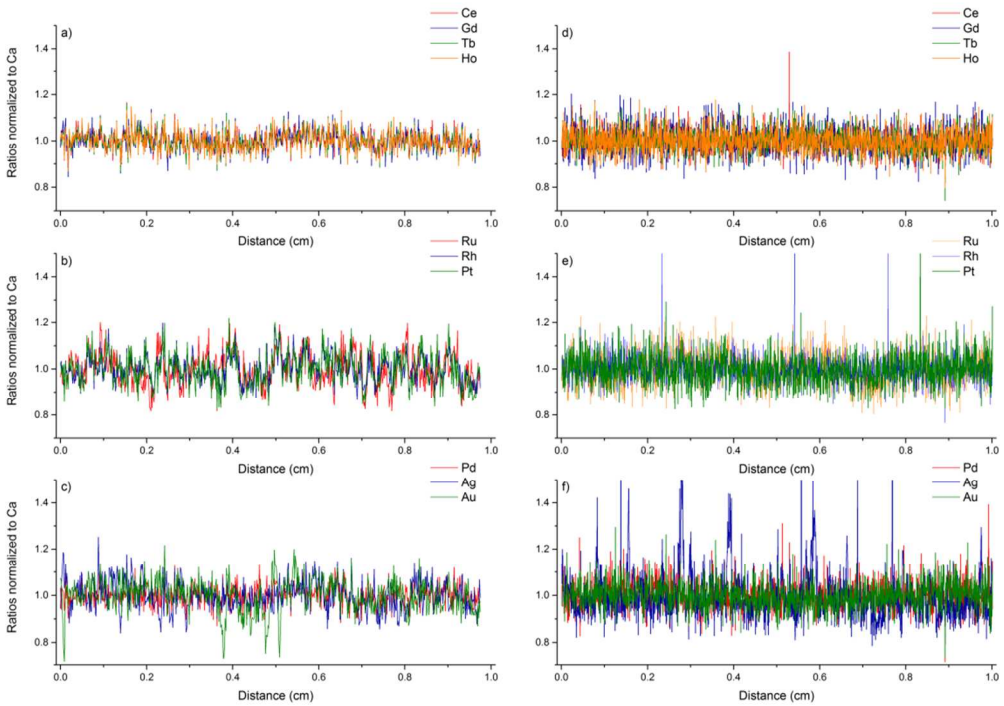

Fig. 2 Variations of elemental responses relative to Ca along a line scan across the sample ablated with a 47 µm beam at UTAS (a-c) on the left hand side and for a 40 µm beam (d-f) at ETH. All individual sweep readings are shown for each element plotted. Ca count rates were used to derive point to point normalization. Normalisation to the average ratio along the scan was performed. Note that REE (plot a and d) show less variations than PGE, Ag and Ag (plots b, c, e, f). Variations in Pt, Rh and Ru (plot b and e) are correlated suggesting that they are present in the same particles which are not evenly distributed, whereas Pd, Au and Ag do not display a correlated pattern.

Ablating the material in single spot mode, it was found that silver seems also to be enriched at the surface of the pressed pellet, which can be seen from its intensity slowly decreasing with progressing ablation depth (supplement information). Due to the already discussed contamination problems it is not possible to discuss this effect conclusively. All the other elements show variations with an uncertainty significantly below the commonly observed RSDs for powder ablations reported in the literature. For example, analytical precision for five replicates on powder samples have been reported to be *e.g.* up to 20 %.[36] The single spot analyses carried out using different crater sizes show that the PGE/Ca ratios are independent of crater size. However, down-hole fractionation or laser-induced fractionation effects and their influence on quantitative analysis were not investigated within this study, since no other PGE-bearing microanalytical reference materials were available.

Table 3 RSDs of intensity ratios determined by linescan data from both laboratories.

Element	Isotope used	RSD of intensity ratio ETH	RSD of intensity ratio UTAS
Na	23	4.9	4.3
Mg	25	5.2	4.1
Al	27	4.2	3.8
Si	29	5.2	3.8
Ti	47	5.3	3.4
Fe	57	5.1	3.9
Ru	101	7.0	7.3
Rh	103	5.8	5.8
Pd	105	6.2	4.5
Ag	107	16.4	6.3
Ce	140	4.9	4.2
Gd	157	6.1	4.5
Tb	159	4.7	4.2
Ho	165	5.1	4.4
Pt	195	6.8	7.0
Au	197	5.9	7.0
Pb	208	12.1	12.8

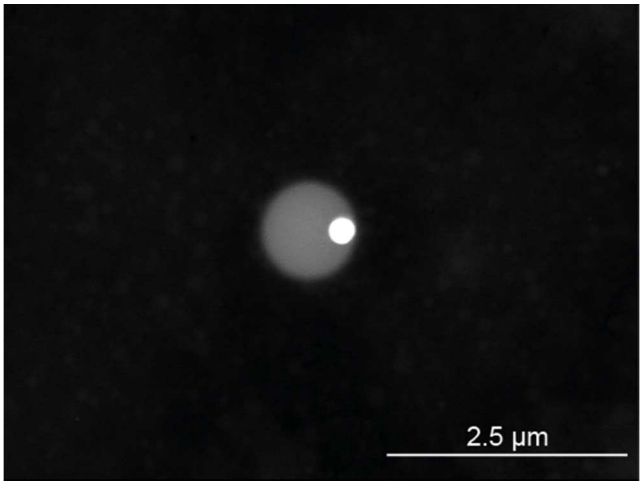

Fig. 3 FE-SEM image for a selected area (black represent the matrix, grey a particle in the matrix), showing a larger bright round particle which contains elevated levels of Pt and Pd on top of larger round grey particle, which is rich in titanium.

To assess the suitability of the material for quantitative analysis, the average error of individual analysis (1 σ) was compared to the relative standard deviation (1 σ) of n=8 at ETH and n=10 at UTAS determinations by laser ablation with different spot sizes according to ref[37]. If the estimation

of error is accurate, a homogenously distributed element should plot on the one to one line, or below (Fig. 4).

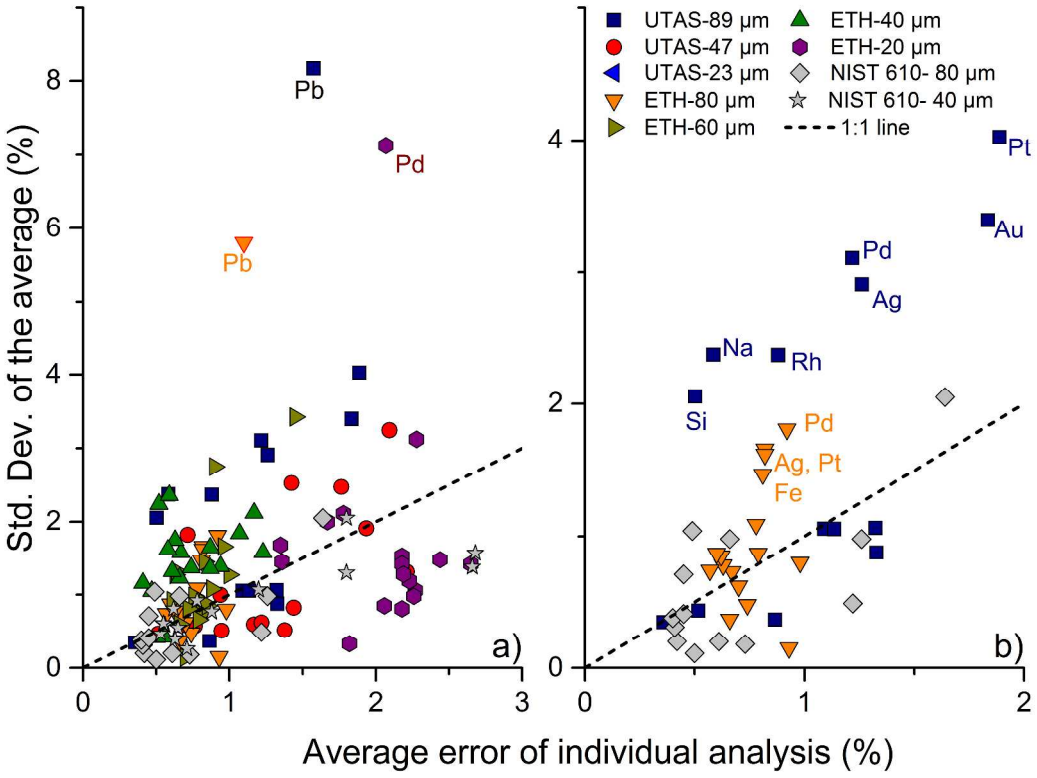

Fig. 4 a) Homogeneity of compacted nanoparticles assessed on the basis of n=8 LA-ICP-MS spot analyses at different crater sizes 20, 40, 60, and 80 µm measured at ETH and 23, 47 and 80 µm measured at UTAS. The distribution of an element is considered to be homogenous, when the variance of the concentration determination is less or equal to the standard error of the analytical measurement. All elements but Pd and Pb, are distributed homogeneously within this newly obtained material. Data for internationally accepted reference materials (NIST SRM 610) are also shown in this plot for comparison. Those data was acquired using 40 and 80 µm spots and the number of determinations was n=4. b) shows data for 80 µm and 89 µm only.

Most elements plot along the one to one line, suggesting a homogenous distribution regardless of the crater size used. However, variations for Pd were detected at 20 µm crater sizes. Supporting the information obtained by the normalized intensity ratio plot (Fig. 2), Pb was found to inhomogenously distributed at 80 µm spot sizes with a RSD greater than 6 %. All other elements have RSDs smaller than 4%, which is considered acceptable for quantification of LA-ICP-MS[38]. It can also be seen in (Fig. 4) that PGE, Au, Pb and Ag are differently distributed than the lithophile elements, which is supported by the occurrence of nanonuggets. It has to be stressed that PGE, Ag and Au were implemented in this proof-of-concept study at unusual high concentrations as those elements are normally found in lower concentration levels. Those non-lithophile elements (PGE and metals) could be implemented in lower concentrations thus achieving a higher amount of mixing with the matrix, which could result in fewer spikes.

4 Conclusion and Outlook

Microbeam techniques require a broader access to calibration materials for quantitative analysis with similar matrices to the sample of interest. Some elements, such as the PGEs have been difficult to be implemented into fused samples. The mixing of powders has been extensively investigated as a possibility to generate calibration materials, however it was shown that different phases remain unmixed and cause deviations, in particular when working with beam diameters in the order of 20 μm and below.

This study presents preliminary results for a newly synthesized calibration material using flame spray synthesis, which is closely matched to the NIST SRM glass 610 which is one of the most used calibration material in LA-ICP-MS. Elements such as Mg, Ti, Fe were added to the matrix in the wt% range and PGE and REE's were added to study the suitability of the spray flame synthesis for incorporation incompatible elements into silicates. By spray combustion of a solution containing precise amounts of the desired metals and subsequent ultra-fast cooling of the formed nanoparticles, so-called *solid solutions* are formed. The data shown in this manuscript indicate that (i) a sufficient high concentration of PGEs can be incorporated into the generated nano-material; (ii) the material can be compacted without any addition of binders; (iii) element ratios deviate significantly less compared to pressed powder analysis; (iv) eliminating contamination during production is critical; and (v) formation of enriched nanoparticles containing PGE's cannot be completely prevented. However, the latter is significantly reduced compared to other production methods.

The characterization shown in this study is by far not as extensive as required to use the material for primary calibrations during routine analysis by LA-ICP-MS. However, the information provided here indicates that flame spray synthesis is capable of producing calibration materials. The major advantage of this technique is that the composition can be designed and up to several 100 g can be sprayed in one batch.

The preliminary data on the silicate glass powder demonstrate that compacted nanoparticles meet the requirement of external calibration materials in LA-ICP-MS. As shown for the REE's, Ti and Mg, customized production of reference materials with a similar quality as reported for NIST glass is possible. However, the data observed for Ag, Pb and PGE's also indicate that some of the production steps need to be investigated at all different productions steps involved (including precipitation during mixing of the precursors, pressing of the pellets, recrystallization/segregation at the nanoparticle level and stability of the pellets as a function of storage conditions such as humidity

and temperature, and time) and are part of ongoing studies. Furthermore, the entire setup for generating future material needs exceptional cleaning to avoid carry over effects caused by previous productions.

5 Acknowledgement

The authors acknowledge Swiss National Science Foundation for funding this research project (SNF Sinergia, Project STALCLIM, SNF Project CRSI22_132646). LD acknowledges the support of the Australian Research Council and Newcrest Mining Limited through funding to the Centre of Excellence in Ore Deposits. DT thanks Dr. H. Wiltsche (TU Graz) for his help in developing the digestion procedure. Dr. Karsten Goemann from the Central Science Laboratory at UTAS and Dr. Frank Krumeich from the Laboratory of Inorganic Chemistry at ETH are thanked for assistance with SEM analyses.

6 Bibliography

1. J. S. Kane, *Geostand. Geoanalytical Res.*, 1998, **22**, 15–31.

2. M. Guillong, K. Hametner, E. Reusser, S. A. Wilson, and D. Günther, *Geostand. Geoanalytical Res.*, 2005, **29**, 315–331.

3. S. Jackson, H. Longerich, G. Dunning, and B. Fryer, *Can. Mineral.*, 1992, **30**, 1049–1064.

4. B. Fryer, S. Jackson, and H. Longerich, *Can. Mineral.*, 1995, **33**, 303–312.

5. J. S. Kane, *Geostand. Newsl.*, 1998, **22**, 7–13.

6. J. S. Kane, *Geostand. Geoanalytical Res.*, 2002, **26**, 7–29.

7. N. J. G. Pearce, W. T. Perkins, J. A. Westgate, M. P. Gorton, S. E. Jackson, C. R. Neal, and S. P. Chenery, *Geostand. Geoanalytical Res.*, 1997, **21**, 115–144.

8. S. M. Eggins and J. M. G. Shelley, *Geostand. Geoanalytical Res.*, 2002, **26**, 269–286.

9. R. W. Hinton, *Geostand. Geoanalytical Res.*, 1999, **23**, 197–207.

10. K. P. Jochum, U. Weis, B. Stoll, D. Kuzmin, Q. Yang, I. Raczek, D. E. Jacob, A. Stracke, K. Birbaum, D. A. Frick, D. Günther, and J. Enzweiler, *Geostand. Geoanalytical Res.*, 2011, **35**, 397–429.

11. A. Rocholl, K. Simon, K. P. Jochum, F. Bruhn, R. Gehann, U. Kramar, W. Luecke, M. Molzahn, E. Pernicka, M. Seufert, B. Spettel, and J. Stummeier, *Geostand. Newsl.*, 1997, **21**, 101–114.

12. Q.-C. Yang, K. P. Jochum, B. Stoll, U. Weis, D. Kuzmin, M. Wiedenbeck, H. Traub, and M. O. Andreae, *Geostand. Geoanalytical Res.*, 2012, **36**, 301–313.

13. K. P. Jochum, U. Nohl, K. Herwig, E. Lammel, B. Stoll, and A. W. Hofmann, *Geostand. Geoanalytical Res.*, 2005, **29**, 333–338.

14. P. Sylvester and S. M. Eggins, *Geostand. Newsl.*, 1997, **21**, 215–229.

15. M. Odegård, J. Mansfeld, and S. H. Dundas, *Fresenius. J. Anal. Chem.*, 2001, **370**, 819–27.

16. R. E. Wolf and S. A. Wilson, *U.S. Geol. Surv. Fact Sheet 2007-3056*, 2007.

17. W. J. Stark, K. Wegner, S. E. Pratsinis, and A. Baiker, *J. Catal.*, 2001, **197**, 182–191.

18. W. J. Stark, L. Mädler, M. Maciejewski, S. E. Pratsinis, and A. Baiker, *Chem. Commun.*, 2003, 588–589.

19. R. Strobel, F. Krumreich, W. J. Stark, S. E. Pratsinis, and A. Baiker, *Chem. Commun.*, 2004, **222**, 307–314.

20. S. Loher, W. Stark, and M. Maciejewski, *Chem. Mater.*, 2005, **1999**, 725–731.

21. R. N. Grass and W. J. Stark, *Chem. Commun.*, 2005, 1767–1769.

22. W. J. Stark and J. D. Grunwaldt, *Chem. Mater.*, 2005, 3352–3358.

23. R. N. Grass and W. J. Stark, *J. Nanoparticle Res.*, 2006, **8**, 729–736.

24. E. K. Athanassiou, R. N. Grass, and W. J. Stark, *Nanotechnology*, 2006, **17**, 1668–1673.

25. T. J. Brunner, R. N. Grass, and W. J. Stark, *Chem. Commun.*, 2006, 1384–1386.

26. M. Rossier, F. M. Koehler, E. K. Athanassiou, R. N. Grass, B. Aeschlimann, D. Günther, and W. J. Stark, *J. Mater. Chem.*, 2009, **19**, 8239–8243.

27. E. K. Athanassiou, R. N. Grass, and W. J. Stark, *Aerosol Sci. Technol.*, 2010, **44**, 161–172.

28. Y. Suzuki, R. Sugita, S. Suzuki, and Y. Marumo, *Anal. Sci.*, 2000, **16**, 1195–1198.

29. S. Gilbert, L. Danyushevsky, P. Robinson, C. Wohlgemuth-Ueberwasser, N. Pearson, D. Savard, M. Norman, and J. Hanley, *Geostand. Geoanalytical Res.*, 2012, **37**, 51–64.

30. H. Longerich, S. Jackson, and D. Günther, *J. Anal. At. Spectrom.*, 1996, **11**, 899–904.

31. R. Mueller, L. Mädler, and S. E. Pratsinis, *Chem. Eng. Sci.*, 2003, **58**, 1969–1976.

32. S. A. Wilson, W. I. Ridley, and A. E. Koenig, *J. Anal. At. Spectrom.*, 2002, **17**, 406–409.

33. C. R. M. Butt and R. B. W. Vigers, *X-Ray Spectrom.*, 1977, **6**, 144–148.

34. J. Graham, C. R. M. Butt, and R. B. W. Vigers, *X-Ray Spectrom.*, 1984, **13**, 126–133.

35. Y. Liu, Z. Hu, S. Gao, D. Gunther, J. Xu, C. Gao, and H. Chen, *Chem. Geol.*, 2008, **257**, 34–43.

36. M. Motelica-Heino and O. Donard, *Geostand. Newsl.*, 2001, **25**, 345–359.

37. L. Danyushevsky, P. Robinson, S. Gilbert, M. Norman, R. Large, P. McGoldrick, and M. Shelley, *Geochemistry Explor. Environ. Anal.*, 2011, **11**, 51–60.

38. K. P. Jochum, B. Stoll, K. Herwig, M. Willbold, A. W. Hofmann, M. Amini, S. Aarburg, W. Abouchami, E. Hellebrand, B. Mocek, I. Raczek, A. Stracke, O. Alard, C. Bouman, S. Becker, M. Dücking, H. Brätz, R. Klemd, D. de Bruin, D. Canil, D. Cornell, C.-J. de Hoog, C. Dalpé, L. Danyushevsky, A. Eisenhauer, Y. Gao, J. E. Snow, N. Groschopf, D. Günther, C. Latkoczy, M. Guillong, E. H. Hauri, H. E. Höfer, Y. Lahaye, K. Horz, D. E. Jacob, S. a. Kasemann, A. J. R. Kent, T. Ludwig, T. Zack, P. R. D. Mason, A. Meixner, M. Rosner, K.

Misawa, B. P. Nash, J. Pfänder, W. R. Premo, W. D. Sun, M. Tiepolo, R. Vannucci, T. Vennemann, D. Wayne, and J. D. Woodhead, *Geochemistry, Geophys. Geosystems*, 2006, **7**, art. no. Q02008.